

## Accretion and Outflow Traced by H<sub>2</sub>O Masers in the Circinus AGN

L. J. Greenhill, J. M. Moran

*Harvard-Smithsonian Center for Astrophysics, 60 Garden St,  
Cambridge, MA 02138 USA*

R. S. Booth

*Onsala Space Observatory, SE-43992 Onsala, Sweden*

S. P. Ellingsen, P. M. McCulloch

*University of Tasmania, Discipline of Physics, GPO Box 252-21,  
Hobart, TAS 7001 Australia*

D. L. Jauncey, R. P. Norris, J. E. Reynolds, A. K. Tzioumis

*Australia Telescope National Facility, PO Box 76, Epping, NSW 2121  
Australia*

J. R. Herrnstein

*Renaissance Technologies, 600 Route 25A, E. Setauket, NY 11733 USA*

**Abstract.** The first VLBI images of H<sub>2</sub>O maser emission in the Circinus Galaxy AGN show both a warped, edge-on accretion disk and an outflow 0.1 to 1 pc from the central engine. The inferred central mass is  $1.3 \times 10^6 M_{\odot}$ , while the disk mass may be on the order of  $10^5 M_{\odot}$ , based on a nearly Keplerian rotation curve. The bipolar, wide-angle outflow appears to contain “bullets” ejected from within  $< 0.1$  pc of the central mass. The positions of filaments and bullets observed in the AGN ionization cone on kpc-scales suggest that the disk channels the flow to a radius of  $\sim 0.4$  pc, at which the flow appears to disrupt the disk.

### 1. Introduction

At a distance of  $\sim 4$  Mpc (Freeman *et al.* 1977) the Circinus galaxy is one of the nearest Seyfert II galaxies that hosts an extragalactic H<sub>2</sub>O maser. The  $3 \times 10^{42}$  erg s<sup>-1</sup> (2-10 keV) central engine is obscured at energies below 10 keV by a large gas column,  $n_{\text{H}} \sim 4 \times 10^{24}$  cm<sup>-2</sup> (Matt *et al.* 1999). Veilleux & Bland-Hawthorn (1997) observed linear optical filaments and compact knots in the ionization cone, which opens by at least 90° at a mean position angle (PA) of roughly 290°. The AGN also drives a kpc-scale nuclear outflow that creates bipolar radio lobes at PA  $\sim 295^\circ$  (Elmouttie *et al.* 1998), largely along the rotation axis of a nuclear <sup>12</sup>CO ring (Curran *et al.* 1998).

There is good evidence that extragalactic H<sub>2</sub>O masers in NGC 4258 and NGC 1068 trace edge-on accretion disks bound by central engines  $\gtrsim 10^6 M_{\odot}$ . Discovery of maser emission in Circinus more or less symmetrically bracketting the systemic velocity led to speculation that these masers also trace an accretion disk (Greenhill *et al.* 1997). Though the detection of an accretion disk reported here confirms that prediction, the additional discovery of qualitatively new, nondisk emission introduces a fresh element in modeling the AGN dynamics.

## 2. Observations and Data

We observed the Circinus H<sub>2</sub>O maser three times in 1997 (June & July) and 1998 (June) with four stations of the ATNF Long Baseline Array. We used a spectral-channel separation of 0.21 km s<sup>-1</sup> over 437 km s<sup>-1</sup> in 1997 and 553 km s<sup>-1</sup> in 1998, centered on the known emission. We calibrated the data with standard VLBI techniques and estimated a new astrometric position for the 565 km s<sup>-1</sup> line (where we adopt the radio astronomical definition of Doppler shift) by analyzing the time variation in fringe rate. The new position,  $\alpha_{2000} = 14^{\text{h}}13^{\text{m}}09^{\text{s}}.95 \pm 0^{\text{s}}.02$ ,  $\delta_{2000} = -65^{\circ}20'21''.2 \pm 0''.1$  is the best estimate so far of the AGN.

We calibrated tropospheric path-length fluctuations by self-calibrating the  $\sim 565$  km s<sup>-1</sup> emission and achieved 0.025 - 0.045 Jy noise ( $1\sigma$ ) in the deconvolved synthesis images, depending on the epoch. We fitted a 2-D Gaussian model brightness distribution to each spot stronger than  $6\sigma$ . Because spectral lines come and go from epoch to epoch, we superposed the maps for all epochs, so as to trace the underlying dense molecular gas as completely as possible with the available data (Figure 1).

## 3. The Warped Disk and Outflow

At each epoch, the sky distribution of maser emission comprises three populations: (1) a thin, gently curved, S-shaped locus of highly redshifted and blueshifted emission arcs to the southwest and northeast, respectively (aka “high-velocity” emission), (2) emission close to the nominal systemic velocity of the galaxy that lies between the high-velocity arcs (aka “low-velocity” emission), and (3) modestly Doppler shifted emission broadly distributed in knots that lie north and west (redshifted) and south and east (blueshifted) of the low-velocity emission. In 1998 detectable emission lay between 215 km s<sup>-1</sup> and 677 km s<sup>-1</sup>.

We have fitted a model edge-on disk with smoothly varying position angle as a function of radius (Figure 1). The observed disk inner and outer radii are  $\sim 0''.005$  and  $\sim 0''.02$ , respectively (0.1 - 0.4 pc). The peak orbital speed is 237 km s<sup>-1</sup>, and the mass enclosed with 0.1 pc is  $1.3 \pm 0.1 \times 10^6 M_{\odot}$ , for circular motion and a 451 km s<sup>-1</sup> model systemic velocity. Among the redshifted high-velocity masers, the peak rotation velocity as a function of impact parameter from the dynamical center,  $b$ , traces a rotation curve that declines as approximately  $b^{-0.40 \pm 0.02}$  (Figure 2). We infer a disk mass on the order of  $10^5 M_{\odot}$  between 0.1 and 0.4 pc. The inner disk is edge-on, but if it is inclined

toward the outer radius, then the disk mass is larger. An estimate of the Toomre Q-parameter ( $\lesssim 0.4$ ) suggests that self-gravity in the disk is important, which is consistent with apparent clumpy substructure in the distribution of disk emission.

The disk model derives its strongest support from the following observations: (1) the angular distribution of high-velocity masers is highly elongated, roughly symmetric, and perpendicular to the approximate axis of the known ionization cone, (2) the apparent rotation curve is nearly Keplerian, (3) the innermost red and blue-shifted emission and the low-velocity emission are colinear in position and position-velocity space. The latter item indicates the low-velocity emission lies close to the inner radius of the disk.

Outflow is traced by emission between 300 and 450 km s<sup>-1</sup>, south and east of the dynamical center of the disk, and by emission between 450 and 580 km s<sup>-1</sup>, north and west of the dynamical center. The distribution of masers on the sky suggests a wide-angle flow, and the segregation of red and blueshifted emission suggests an inclined flow. Because H<sub>2</sub>O maser emission requires  $n_{\text{H}_2} \gtrsim 10^9 \text{ cm}^{-3}$ , the masers probably represent high-density “bullets” immersed in a thinner, photoionized medium, equivalent to a narrow-line region. However, the opacity of that region probably obscures all but the nearside of the flow, and if the disk is inclined toward its outer radius, then ionization along the disk surface probably obscures one side of the flow preferentially.

The outflow appears to arise in the vicinity of the central engine ( $< 0.1 \text{ pc}$ ) rather than from the “maser-disk” by magneto-centrifugal processes (Emmering *et al.* 1992; Kartje, Königl, & Elitzur 1999). Notably, rotation is absent from the line-of-sight velocity and position data, even for masers quite close to the disk (i.e., height/radius  $\ll 1$ ). Though the outflow could originate in a “hot” disk that lies within the (warm) molecular maser-disk, the physical conditions that support maser emission are consistent with adiabatic expansion of AGN broad line clouds, i.e.,  $10^{10} - 10^{12} \text{ cm}^{-3}$  and of  $10^4 \text{ K}$  (Brotherton *et al.* 1994).

The disk structure disappears at a radius of  $\sim 0.4 \text{ pc}$  (Figures 1 & 2), perhaps because the wind disrupts the accretion disk, whose mean surface density presumably declines with increasing radius. The existence of an outer radius is supported circumstantially by two observations. First, outflow-borne masers all lie at the edge of or outside the shadow cast by the truncated disk. (We assume that the maser excitation depends on irradiation and heating of molecular gas by hard X-rays, as in Neufeld, Maloney, & Conger (1994)). Second, the position angles at which the outflow is free of occultation by the truncated disk coincide with the limits of the kiloparsec scale ionization cone observed west of the nucleus (Veilleux & Bland-Hawthorne 1997). For example, the southern edges of the redshifted maser outflow and the ionization cone, both lie at position angles of  $\sim -120^\circ$ . In addition, we note that the mean axis of the maser outflow,  $-52^\circ$ , corresponds well to the orientation of the dominant [O III] filament,  $\sim -50^\circ$  and a radio hotspot (Elmouttie *et al.* 1998).

## References

- Brotherton, M. S., Wills, B. J., Francis, P. J., Steidel, C. C. 1994, *ApJ*, 430, 495  
 Curran, S., Johansson, L., Rydbeck, G., Booth, R. 1998, *A&A*, 338, 863

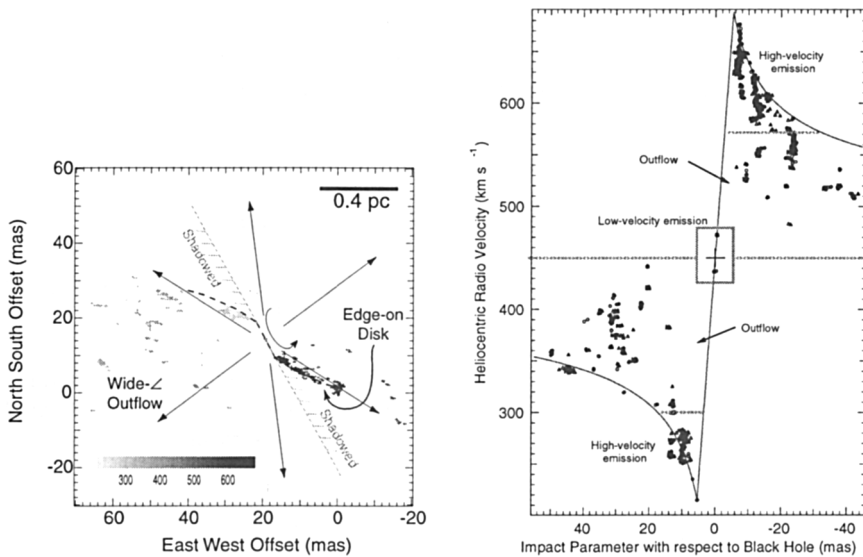


Figure 1. (*left*) A model of the proposed disk-outflow structure in the inner 1 pc of the AGN overlaid on the combined distributions of maser spots observed at three epochs (registered with 0.2 mas accuracy). Shading of spots indicates line-of-sight velocity, and error bars indicate total ( $1\sigma$ ) position uncertainties. Dashed lines trace the warped edge-on disk. Outward facing arrows indicate the wide-angle outflow. The disk shadows some regions, which cannot support maser emission probably because they are not irradiated by the central engine. Synthesized beams appear in the lower left corner. (*right*) Position-velocity diagram annotated to highlight the proposed disk and outflow components. Dashed rotation curves correspond to the midline of the disk. The steep diagonal line corresponds to the near side of the disk, at the inner radius. The outflow is Doppler shifted with respect to the systemic velocity by on the order of  $\pm 100 \text{ km s}^{-1}$ .

- Emmering, R. T., Blandford, R. D., Shlosman, I. 1992, *ApJ*, 385, 460  
 Freeman, K. C., Karlsson, B., Lynga, G., Burrell, J. F., van Woerden, H., Goss, W. M., Mebold, U. 1977, *A&A*, 55, 445  
 Greenhill, L. J., Ellingsen, S. P., Norris, R. P., Gough, R. G., Sinclair, M. W., Moran, J. M., Mushotzky, R. 1997, *ApJ*, 474, L103  
 Jones, K. L., Koribalski, B. S., Elmouttie, M., & Haynes, R. F. 1999, *MNRAS*, 302, 649  
 Kartje, J. F., Königl, A., Elitzur, M. 1999, *ApJ*, 513, 180  
 Matt, G., *et al.* 1999, *A&A*, 341, L39  
 Neufeld, D. A., Maloney, P. R., Conger, S. 1994, *ApJ*, 436, L127  
 Veilleux, S., Bland-Hawthorn, J., 1997 *ApJ*, 479, L105